Available online at www.sciencedirect.com
SCIENCE DIRECT®
Journal of Molecular Catalysis A: Chemical 222 (2004) 243–251
JOURNAL OF MOLECULAR CATALYSIS A: CHEMICAL
www.elsevier.com/locate/molcata

Correlating the electronic properties and HDN reactivities of organonitrogen compounds: an ab initio DFT study

Mingyong Sun[a], Alan E. Nelson[a,*], John Adjaye[b]

[a] *Department of Chemical and Materials Engineering, University of Alberta, Edmonton, Alta., Canada T6G 2G6*
[b] *Syncrude Canada Ltd., Edmonton Research Centre, Edmonton, Alta., Canada T6N 1H4*

Received 6 July 2004; received in revised form 12 August 2004; accepted 12 August 2004
Available online 13 September 2004

Abstract

The electronic structures and properties of representative organonitrogen compounds present in crude oil have been calculated using density-functional theory (DFT) under generalized gradient approximation (GGA). These basic and non-basic organonitrogen compounds have distinct electronic structures and properties that determine their HDN reactivities on hydrotreating catalyst surfaces. The HDN reactivities of cyclohexylamines and piperidines can be correlated to the Mulliken charges on the nitrogen atoms of the organonitrogen molecules, and the hydrogenation activities of aromatic molecules can be correlated to the highest occupied π-orbitals or lowest unoccupied π-orbitals depending on the electronic structure of the catalyst surface. Adjusting electronic structures of hydrotreating catalysts by insightful incorporation of select promoters will change catalyst HDN selectivity for the hydrotreatment of basic and non-basic nitrogen compounds.

Keywords: Hydrotreating; Hydrodenitrogenation; Hydrogenation; Density-functional theory; Organonitrogen; Electronic structures

1. Introduction

As the supply of light crude oil is consumed, the need to upgrade heavy oil and vacuum residue to middle and light distillates will become increasingly important. This upgrading process involves simultaneous catalytic reactions to remove sulfur and nitrogen heteroatoms, as well as selective hydrogenation to produce high-quality distillates and clean burning fuels. The hydrodenitrogenation (HDN) of heavy oils and bitumens is a primary interest because these crude oils typically have higher total nitrogen content compared to light crude oils. Organonitrogen compounds must be removed from petroleum for several key reasons, including to minimize the poisoning of noble metal and acidic catalysts and to meet stringent product quality regulations [1–3]. The development and optimization of HDN catalysts requires an acute knowledge of the structure–property relationship of organonitrogen compounds and hydrotreating catalyst surfaces. Therefore, understanding the correlations between the electronic structures and properties of organonitrogen molecules and their reactivities on hydrotreating catalysts is an important step towards the successful development of new catalysts with higher activity and selectivity for HDN reactions.

In crude oil, most of the nitrogen is present in the form of heterocyclic unsaturated compounds having five-membered (non-basic) pyrrolic rings or six-membered (basic) pyridinic rings, and a small amount in the form of aliphatic amines or anilines [3,4]. To remove nitrogen atoms from organonitrogen molecules, the cleavage of C–N bonds is an essential step. Depending on the type of carbon atom to which the nitrogen atom is bonded, there are two types of C–N bonds: C(sp^2)–N represented by unsaturated heterocyclic or aniline type molecules, and C(sp^3)–N represented by saturated heterocyclic or non-heterocyclic amines. Generally, complete saturation of the carbon atom is necessary to cleave the C(sp^2)–N bond on sulfide catalysts, and eventually the

* Corresponding author. Tel.: +1 780 492 7380; fax: +1 780 492 2881.
E-mail address: alan.nelson@ualberta.ca (A.E. Nelson).

1381-1169/$ – see front matter © 2004 Elsevier B.V. All rights reserved.
doi:10.1016/j.molcata.2004.08.015

nitrogen atom is removed via C(sp^3)–N bond cleavage [5]. While it is accepted C(sp^3)–N bond cleavage occurs via Hofmann-type elimination and/or nucleophilic substitution on conventional hydrotreating catalysts as first suggested by Nelson and Levy [6], detailed investigations of the mechanism of C–N bond cleavage have been the focus of many studies [7–17]. Recently published results indicate that the dominant mechanism for HDN depends on the structures of the organonitrogen molecules [16,17].

The objective of the present study is to correlate the electronic properties and structures of organonitrogen and aromatic compounds to hydrotreating reactivity. In the first part, the HDN reactivities of cyclohexylamines and piperidines and hydrogenation reactivities of aromatics are correlated to their electronic properties. In the second part, the electronic structures and properties of basic and non-basic heterocyclic organonitrogen compounds found in crude oils are calculated, and their implications to HDN catalysis are discussed. This approach provides additional insight into the C–N bond cleavage mechanism and further information regarding the possible role of catalytic active sites on hydrotreating catalyst surfaces.

2. Computational method

Molecular geometry optimization and energy calculations are based on density-functional theory (DFT), and have been performed using Material Studio DMol^3 (version 2.2) from Accelrys® [18]. The same software package has been used in calculating surface structures of MoS_2 [19] and WS_2-based [20] hydrotreating catalysts. The electronic wavefunctions are expanded in numerical atomic basis sets defined on an atomic-centered spherical-polar mesh. The double-numerical plus polarization functions (DNP) all electron basis set and Becke exchange [21] plus Perdew correlation [22] non-local functionals (GGA-BP) are used in all calculations. The real space cutoff radius is 4.5 Å. The Kohn–Sham equations [23] are solved by a self consistent field (SCF) procedure. The convergence criterion for the SCF cycle is set at 0.00001. The geometry optimization (atom relaxation) convergence thresholds for energy change, maximum force, and maximum displacement between optimization cycles are 0.00002 Ha, 0.004 Ha/Å, and 0.005 Å, respectively. Techniques of direct inversion in an iterative subspace (DIIS) [24] with a size value of 6, thermal smearing, and a range of 0.005 Ha are applied to accelerate convergence.

The catalyst surface structures stable at reaction conditions for unpromoted and nickel-promoted catalysts are taken from our previous work [19]. Fig. 1 is the catalyst model used in CASTEP calculations, consisting of one layer of nickel atoms at the edge surface. For the unpromoted MoS_2 catalyst, the top layer is molybdenum covered by adsorbed sulfur atoms [19]. In this model, the unit supercell is repeated in *y*-direction with a periodicity of two S–Mo–S units and separated by a vacuum layer of 15 Å in both the *z*- and *x*-directions. The volume of the unit supercell is 18.4 Å × 6.3 Å × 24.6 Å. The electronic structures and total energy calculations for these catalyst surfaces have been performed using Material Studio CASTEP (Cambridge Sequential Total Energy Package) from Accelrys® (version 2.2) based on DFT total energy plane-wave pseudopotential methods [25]. The wave functions of valence electrons are expanded in a plane wave basis set with a Monkhorst–pack *k-point* of (1 × 3 × 1) within a kinetic cutoff energy of 270 eV. Core electrons are represented by non-local ultra-soft pseudopotentials (USP). Generalized gradient corrected PW91 functional was used to calculate the non-local exchange-correlation contribution to the total electronic energy (GGA-PW91) [26]. The SCF convergence criterion for the energy calculation is set at 2 × 10^{-6} eV/atom.

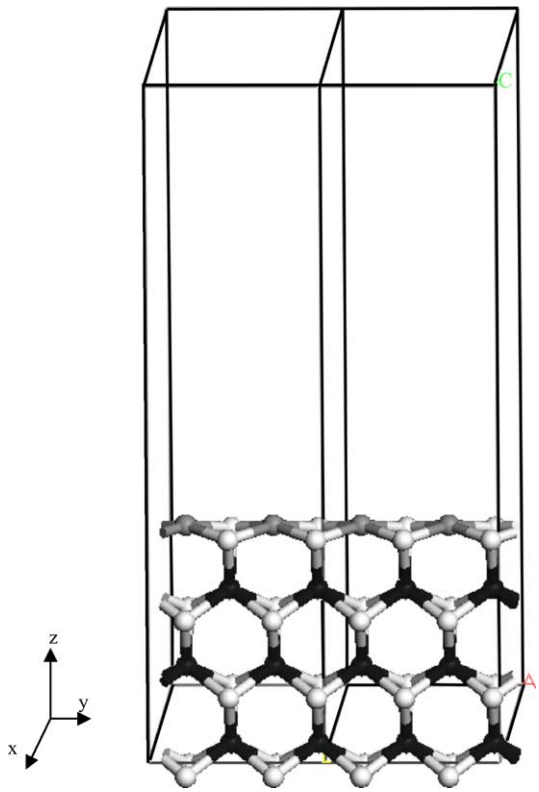

Fig. 1. Catalyst model showing the unit cell and vacuum space above the edge surface. Black balls: molybdenum atoms, light grey: sulfur, dark grey: nickel atoms.

3. Results and discussion

3.1. Correlations between electronic properties and HDN reactivities of cyclohexylamines and piperidines

In the HDN of aniline type compounds, approximately 90% of the conversion is achieved by hydrogenation of the aromatic ring followed by the HDN of cyclohexylamines [5]. Similarly, in the HDN of pyridine the nitrogen atom is removed through the hydrogenation of the heterocyclic

ring followed by the HDN of piperidine [5,27]. In the HDN of cyclohexylamines [13] and piperidines [10,15], the presence of methyl groups at different positions around the saturated molecular ring affects the HDN reactivities. Explanations have been given to account for the effects of the methyl groups on reactivities of these nitrogen-containing compounds [10,13,15]. In order to provide additional insight to explain the effect of methyl group substitution, the reactivities of these compounds on $NiMo/Al_2O_3$ hydrotreating catalysts are correlated to their electronic properties. The electronic properties of cyclohexylamines and piperidines are obtained by ab initio DFT calculations, and their HDN reactivity data are taken from references [13,15], respectively.

Fig. 2 shows the correlations of the HDN reactivities of the cyclohexylamines and the negative Mulliken charges on the nitrogen atom of the corresponding molecules. The HDN reactivities of cyclohexylamines on sulfided $NiMo/Al_2O_3$ increase with the presence of a methyl group at the 2- and 6-positions [13]. Ab initio DFT calculations indicate that the substitution of the hydrogen atoms at the 2- and 6-positions of cyclohexylamine by methyl groups increases the negative Mulliken charges on the nitrogen atom. An excellent correlation between the HDN reactivity and negative Mulliken charges on the nitrogen atom is also observed for substituted piperidines (Fig. 3). The density matrix and atomic overlap matrix are used to partition charge among the atoms [28].

Considering $C(sp^3)$–N bond cleavage followed Hofmann-type elimination, Portefaix et al. [10] reported that the HDN reactivities of piperidine, 2-methylpiperidine, and 2,6-dimethylpiperidine increased due to the increase in the number of hydrogen atoms on the β-carbon atoms [10]. In a recent study, Egorova et al. found that the HDN reactivities of piperidines decreased when methyl groups are attached to the piperidine ring at the 2- and 6-positions, which brings additional β-hydrogen atoms [15]. The lower HDN reactivities of the methyl-substituted piperidines were explained by the steric hindrance of the methyl groups for elimination [15] or substitution [17]. The present study provides another possible explanation, specifically the Mulliken negative

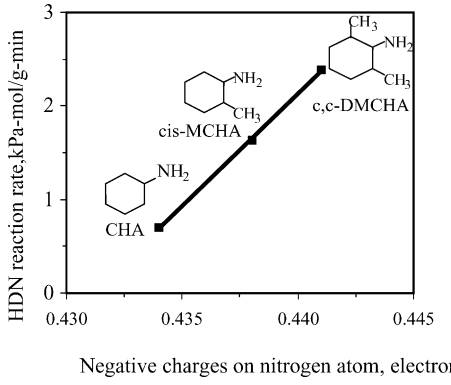

Fig. 2. Correlation between the HDN reactivities of cyclohexylamines on a NiMo catalyst and the negative Mulliken charges on the nitrogen atom. The HDN reaction rates were taken from Ref. [13].

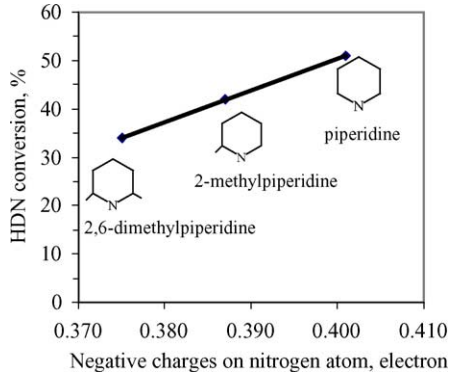

Fig. 3. Correlation between the HDN reactivities of piperidines on a NiMo catalyst and the negative Mulliken charges on the nitrogen atom. The HDN conversion data were taken from Ref. [15].

charge on the nitrogen atom determines the HDN reactivities of the piperidines.

The steric hindrance of the methyl group fails to explain the relative HDN reactivities of cyclohexylamine and substituted cyclohexylamines; the molecules with methyl groups at the 2- and 6-positions have higher HDN reactivity [13]. The reactivity order has been explained by stereochemistry [13,17]. However, the Mulliken negative charge on the nitrogen atom can also explain the increase in the HDN reactivities with the presence of methyl groups at the 2- and 6-positions of cyclohexylamine (Fig. 2). The correlation between the Mulliken negative charge on the nitrogen atom and relative HDN reactivities of both piperidines and cyclohexylamines suggests that the electronic structure around the nitrogen atom plays an essential role in determining the intrinsic reactivities of $C(sp^3)$–N bond cleavage.

Regardless of what mechanism is responsible for HDN reactions, the adsorption of the nitrogen molecules on active sites is required. The adsorption of saturated nitrogen molecules on edge surfaces of sulfide catalysts occurs through the nitrogen atom with the electron lone pair bonding to unsaturated metal sites. A higher negative charge on the nitrogen atom of a saturated nitrogen molecule would lead to stronger adsorption of the molecule on the catalyst surface through metal–nitrogen bonding, where unsaturated metal sites on the catalyst surface act as Lewis acids to accept the lone pair of electrons from the nitrogen atom. The stronger adsorption would yield a larger adsorption constant, and thus a higher surface coverage. This might be the reason (or partly) for the excellent correlation between the charge on nitrogen atom and reaction rate. However, if the adsorption constants of all molecules were large enough, the coverage of the nitrogen molecules on the catalyst surface would approach unity at reaction conditions, provided suitable partial pressures of nitrogen molecules above the catalyst surface. In this instance, the difference in adsorption constants would not affect the HDN rate.

A higher charge on the nitrogen atom also indicates a weaker C–N bond. If the cleavage of the C–N bonds in

the nitrogen molecules proceeds along an SN_2 mechanism, the C–N bond would cleave following the adsorption of the nitrogen molecules on active sites through nitrogen–metal bonding and the attack of a nucleophile (presumably surface –SH groups) at the α-C atoms. For an E_2 mechanism, the cleavage of a C–N bond follows the adsorption of the nitrogen molecules and abstraction of β-C–H, which produces alkenes. In both scenarios, a weaker C–N bond instead of larger adsorption energy might be responsible for the higher reaction rate. In order to clearly explain why a linear correlation between charge and rate exists, further investigations are required.

3.2. Correlations between electronic properties and hydrogenation activities of aromatics

The HDN of heterocyclic aromatic and aniline type nitrogen compounds requires the saturation of the heterocyclic or phenyl ring before C–N bond cleavage [5,8]. For hydrogenation reactions, it is logical to examine the correlation between the π-system of the aromatic ring and the hydrogenation reactivities of aromatic molecules. The calculated electronic properties of the π-system for several aromatic compounds and the hydrogenation rates of these aromatic molecules on sulfided unpromoted and nickel-promoted molybdenum catalysts reported by Quartararo et al. [29] are presented in Table 1. DFT calculations show that an increase in the number of methyl groups around the benzene ring increases the energy levels of both the highest occupied molecular orbital (HOMO) and lowest unoccupied molecular orbital (LUMO). The hydrogenation reactivities of the aromatic molecules increase on the sulfided molybdenum catalyst, however, decrease on the sulfided nickel-promoted catalyst with the number of the methyl groups on the aromatic ring. The relative hydrogenation reactivities of the aromatic molecules on catalysts depend not only on the structures of the molecules, but also on the properties of catalyst surfaces.

Previous studies on the surface structures of the sulfided molybdenum and nickel-promoted catalysts indicate that at typical reaction conditions, a bare Ni-promoted edge is stable for a NiMo catalyst and a Mo-edge with about 25–50% sulfur coverage is stable for MoS_2 [19,30,31]. The electronic properties of the unprompted MoS_2 [30] and Ni-promoted edge surfaces [31] with different sulfur coverages have been studied previously. In the present study, the density of states for the unpromoted Mo-edge with 25% sulfur coverage and the bare Ni-edge were calculated using the optimized surface structures obtained in our previous work [19]. Fig. 4a shows the local density of d states projected on the molybdenum site on the partially sulfided Mo-edge, and Fig. 4b the local density of d states projected on the nickel site on the bare Ni-edge; Figs. 4c and d are the corresponding surface structures of unpromoted and nickel-promoted catalysts [19].

The molybdenum site has a low density of occupied states below the Fermi level and a relatively high density of unoccupied states above the Fermi level. Such an electronic structure on the unpromoted molybdenum site indicates the molybdenum sites on MoS_2 catalysts are poor electron donors and good acceptors. When the aromatic molecules react on the molybdenum sites, the electrons from the HOMOs of the molecules transfer to the unoccupied states of the active sites. The higher energy level of the HOMO makes it easier for the molecule to donate electrons. The correlation between the HOMO energy level and hydrogenation activity on the unpromoted molybdenum catalyst indicates that the interactions of the aromatic molecules on the molybdenum sulfide catalysts occur primarily through the donation of electrons from molecules to the catalyst surface. On the bare Ni-edge surface, the nickel site has a high density of occupied states and a low density of unoccupied states, which is completely different from the molybdenum site on the unpromoted catalyst. The electronic structure on the nickel site indicates that the nickel sites on sulfided NiMo catalysts are excellent electron donors and poor acceptors. When the aromatic molecules react on the nickel-promoted edge surface of a NiMo catalyst, the electrons from the catalyst surface transfer to the LUMOs of the molecules. The higher energy level of the LUMO makes it more difficult for the molecule to accept electrons from the catalyst surface. This explains why an increase in number of the methyl groups on the benzene ring decreases the hydrogenation reactivity on the sulfided NiMo catalyst, while it increases the hydrogenation activity on the molybdenum catalyst.

3.3. Electronic properties of organonitrogen compounds present in crude oils

The heterocyclic nitrogen compounds contribute to a major part of the nitrogen content in crude oils, and are more difficult to remove than aliphatic nitrogen compounds [3,4]. Distillates derived from heavy oils and bitumens by conversion processes contain higher amounts of unsaturated hetero-

Table 1
HOMO and LUMO energy levels and hydrogenation reactivities of aromatics on sulfided molybdenum and nickel-promoted molybdenum catalysts

Aromatic compounds	Orbital eigenvalue (eV)		Reaction rates (mol/mol_{metal} h^{-1})	
	HOMO	LUMO	Mo catalyst	NiMo catalyst
Toluene	−5.97	−1.09	2.48	39.59
m-Xylene	−5.80	−1.02	4.60	19.18
1,3,5-Trimethylbenzene	−5.68	−0.91	5.96	10.69
1,2,4,5-Tetramethylbenzene	−5.37	−0.81	6.07	8.03

The reactivity data are taken from Ref. [29].

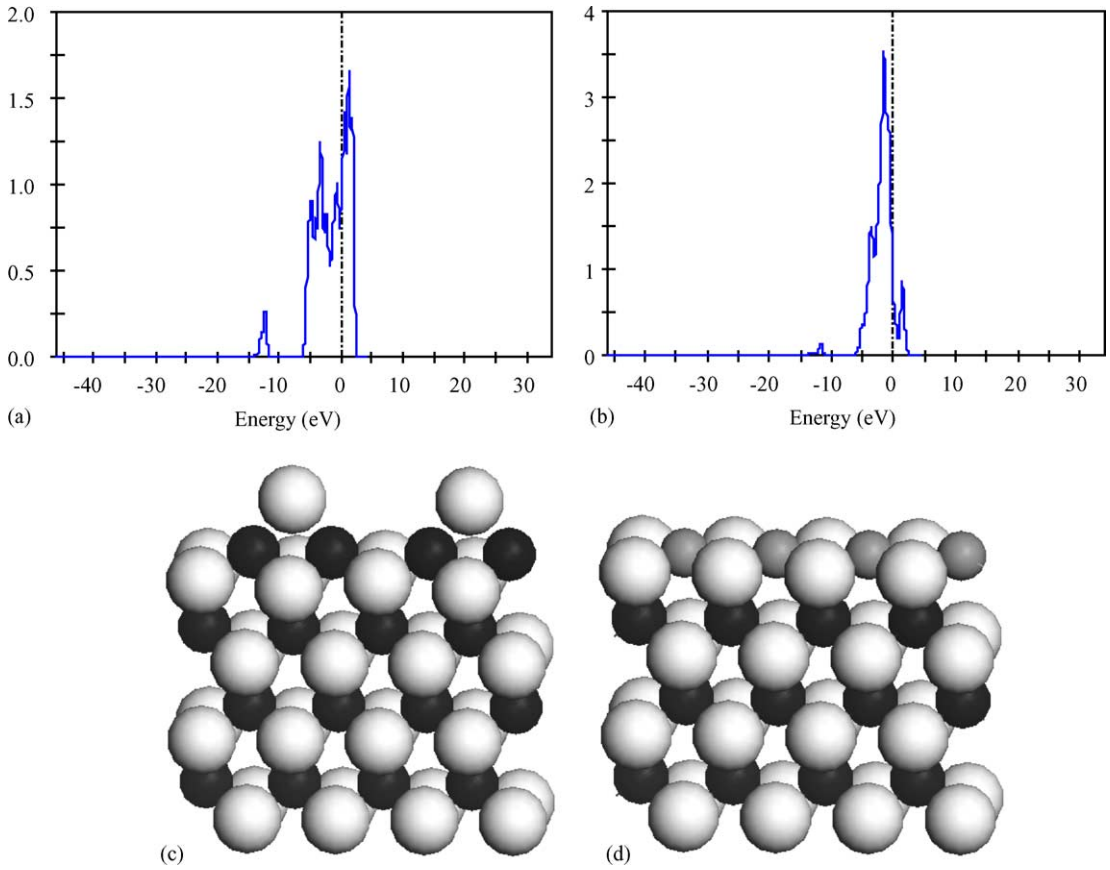

Fig. 4. Densities of d states projected on the surface metal atoms of (a) unpromoted and (b) Ni-promoted surfaces. The corresponding optimized surface structures of (c) MoS_2 Mo-edge with 25% sulfur coverage and (d) bare Ni-edge of the Ni-promoted molybdenum catalyst. Black balls: molybdenum atoms, dark grey: nickel atoms, light grey: sulfur atoms.

cyclic nitrogen compounds, which make it even more difficult to reduce the nitrogen content for these fractions [32]. For the hydrogenation of aromatic heterocyclic nitrogen compounds, which is required for C–N bond cleavage, understanding the energetics and structures of the π-orbitals is required. Additionally, basic and non-basic nitrogen compounds have distinct electronic structures and properties that determine their differences in HDN reactivities on catalyst surfaces.

Pyridine is the simplest six-membered heterocyclic nitrogen compound and is often used as a model compound to test the activity of HDN catalysts. Fig. 5a shows the electrostatic potential field around pyridine. The dark region at the nitrogen atom represents a negative electrostatic potential field, and the light grey region indicates that a positive electrostatic potential field surrounds the plane of the six-member ring. The unsaturated metal atoms, which are active centers on a metal sulfide catalyst surface, are positively charged. Therefore, pyridine will approach the active center with the nitrogen atom pointing to the positively charged metal atoms due to Coulombic attraction. If the pyridine molecule is subject to electrophilic attack on the nitrogen atom by the active species on the catalyst surface, the electrons in its HOMO will contribute to form a new bond with the active species on catalyst surfaces. Fig. 5b shows the shape of the pyridine HOMO, which indicates that the nitrogen atom has the highest probability to form a bond with the catalyst active site. These results predict that an end-on adsorption favors the formation of a strong bond with strong Lewis acid sites (metal sites) on the catalyst surface. This end-on adsorption configuration does not affect the π-electron system of the molecule, and thus contributes little to the hydrogenation of the heterocyclic ring. The LUMO of pyridine will accept electrons to form bonds with active centers on the catalyst. The shape of the pyridine LUMO shows that a side-on configuration of pyridine on the catalyst surface is required in order for pyridine to accept electrons from the catalyst using its LUMO (Fig. 5c).

For quinoline, a phenyl ring is attached to the pyridine ring. The negative electrostatic potential field still concentrates around the nitrogen atom, and the two-ring plane is surrounded by a positive potential field (Fig. 5d). The shapes of the HOMO (Fig. 5e) and LUMO (Fig. 5f) indicate that a side-on adsorption is required to form bonds by accepting or donating electrons through π-system. Figs. 5g–i show the electrostatic potential field, HOMO, and LUMO for acridine, respectively. The side-on adsorption of acridine through the π-system on a catalyst surface is favored by the electronic structures.

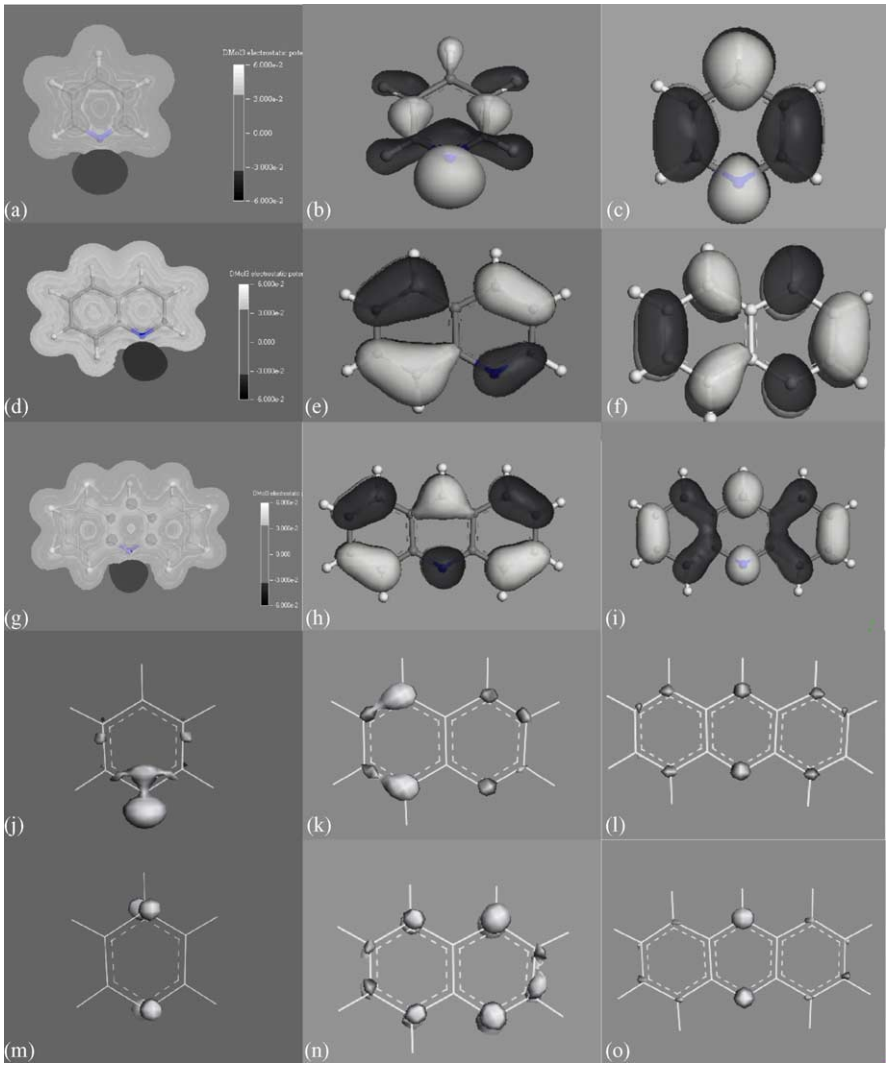

Fig. 5. Electronic structures for basic nitrogen molecules. (a) Electrostatic potential field around pyridine molecule; (b) pyridine highest occupied molecular orbital (HOMO); (c) pyridine lowest unoccupied molecular orbital (LUMO); (d) electrostatic potential field around quinoline molecule; (e) quinoline highest occupied molecular orbital (HOMO); (f) quinoline lowest unoccupied molecular orbital (LUMO); (g) electrostatic potential field around acridine molecule; (h) acridine highest occupied molecular orbital (HOMO); (i) acridine lowest unoccupied molecular orbital (LUMO); (j) electrophilic Fukui function isosurface for pyridine (isovalue = 0.1); (k) electrophilic Fukui function isosurface for quinoline (isovalue = 0.04); (l) electrophilic Fukui function isosurface for acridine (isovalue = 0.04); (m) nucleophilic Fukui function isosurface for pyridine (isovalue = 0.1); (n) nucleophilic Fukui function isosurface for quinoline (isovalue = 0.04); (o) nucleophilic Fukui function isosurface for acridine (isovalue = 0.04).

Fukui functions provide a method of measuring and displaying the reactivity of regions of a molecule for electrophilic attack (losing electrons) or nucleophilic attack (gaining electrons) [33]. Figs. 5j–l show the most reactive regions of pyridine, quinoline, and acridine for electrophilic attack, and Figs. 5m–o show the most reactive regions of the three molecules for nucleophilic attack. For pyridine, the most reactive region for electrophilic attack is at the nitrogen atom favored by end-on adsorption of the molecule through the nitrogen atom on a catalyst surface; the most reactive region for nucleophilic attack is located at the nitrogen atom and the carbon atom at the opposite end (at position 4 relative to the nitrogen atom), favored by side-on adsorption on a catalyst surface. For quinoline, the carbon atoms at the 5- and 8-positions on the phenyl ring are more reactive than the nitrogen atom and carbon atoms at the 3- and 4-positions on the nitrogen ring for electrophilic attack. However, the nitrogen atom and carbon at position 4 on the nitrogen ring is the most reactive region for nucleophilic attack. For acridine, the middle nitrogen ring is more active than the two phenyl rings for both electrophilic and nucleophilic attack. For quinoline and acridine, flat-on adsorption of the molecules on catalyst surface is required for both types of reactions to occur effectively.

Pyrrole is the simplest five-membered ring nitrogen compound, which has a different electronic structure than pyridine. Fig. 6a shows that the molecular plane of pyrrole is surrounded by a positive electrostatic potential field and neg-

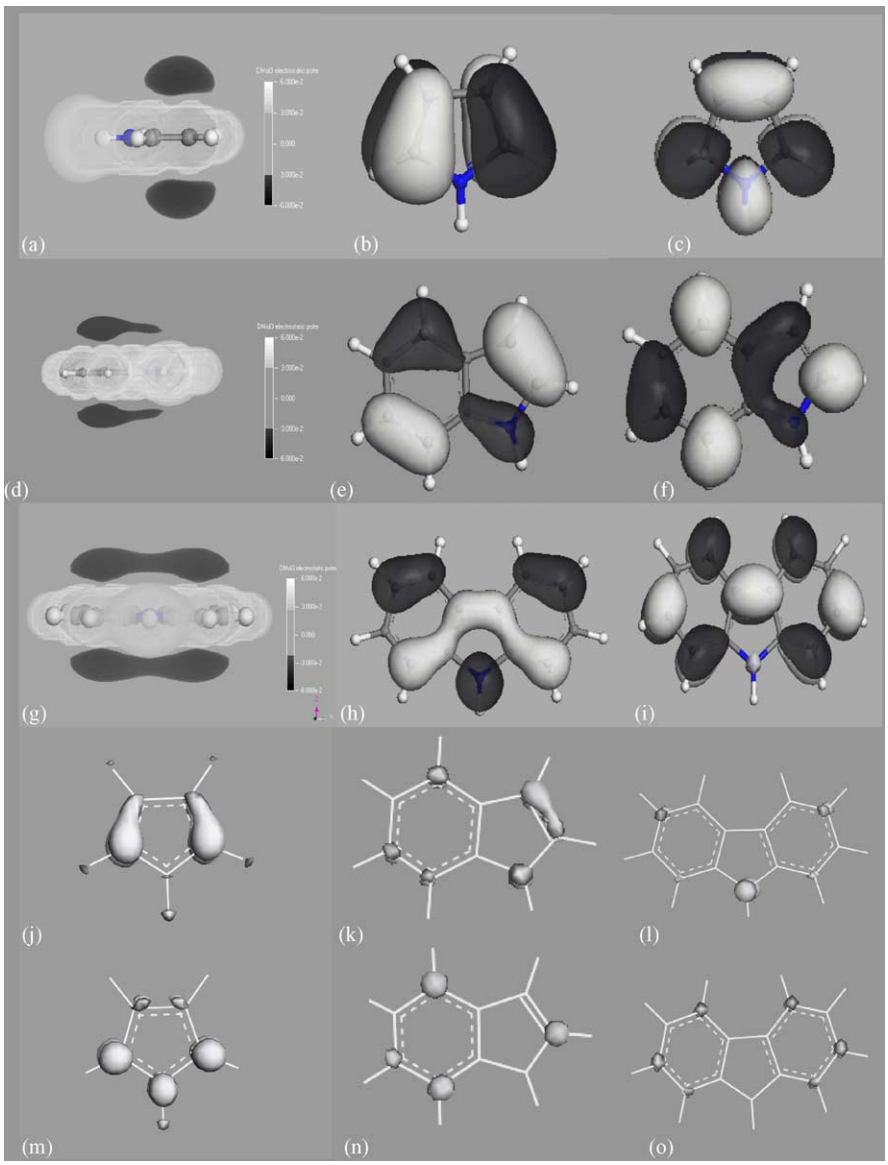

Fig. 6. Electronic structures for non-basic nitrogen molecules. (a) Electrostatic potential field around pyrrole molecule; (b) pyrrole highest occupied molecular orbital (HOMO); (c) pyrrole lowest unoccupied molecular orbital (LUMO); (d) electrostatic potential field around indole molecule; (e) indole highest occupied molecular orbital (HOMO); (f) indole lowest unoccupied molecular orbital (LUMO); (g) electrostatic potential field around cabazole molecule; (h) cabazole highest occupied molecular orbital (HOMO); (i) cabazole lowest unoccupied molecular orbital (LUMO); (j) electrophilic Fukui function isosurface for pyrrole (isovalue = 0.05); (k) electrophilic Fukui function isosurface for indole (isovalue = 0.05); (l) electrophilic Fukui function isosurface for cabazole (isovalue = 0.05); (m) nucleophilic Fukui function isosurface for pyrrole (isovalue = 0.05); (n) nucleophilic Fukui function isosurface for indole (isovalue = 0.05); (o) nucleophilic Fukui function isosurface for cabazole (isovalue = 0.05).

ative potential fields are distributed above and below the molecular plane. The shapes of the HOMO (Fig. 6b) and LUMO (Fig. 6c) indicate that only side-on adsorption of pyrrole on the catalyst surface will lead to reaction by donating or accepting electrons with catalyst surface. For indole, the negative electrostatic potential field concentrates at both sides of the phenyl plane (Fig. 6d). The HOMO (Fig. 6e) and LUMO (Fig. 6f) distribute around both the phenyl ring and the nitrogen ring at both sides the molecular plane. Fig. 6g presents the distribution of the electrostatic potential field around carbazole, and Figs. 6h and i the HOMO and LUMO of carbazole. The bonding probabilities for these multi-ring non-basic molecules are favored by side-on adsorption on the catalyst surface.

Figs. 6j–l show the Fukui function analysis results for electrophilic attack, and Figs. 6m–o for nucleophilic attack on pyrrole, indole, and carbazole, respectively. The most reactive region for electrophilic attack is the 2- and 5-carbon atoms for pyrrole, at the 3-carbon atom for indole, and at the nitrogen atom for carbazole. For nucleophilic attack, the most reactive region is located at the 2- and 5-carbon atoms as well as the nitrogen atom for pyrrole, at 2-, 4-, and 7-carbon

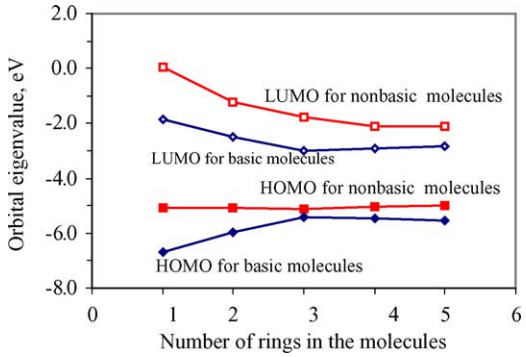

Fig. 7. The energy levels of highest occupied π-orbitals and lowest unoccupied π-orbitals of basic and non-basic nitrogen molecules.

atoms for indole, and at the carbon atoms of the phenyl ring for carbazole.

The first step for the HDN of aromatic heterocyclic nitrogen compounds is the hydrogenation of the aromatic ring, which involves the π-system of the aromatic structure. Thus, the electronic structures and energy levels of the highest occupied π-orbital and lowest unoccupied π-orbital should play important roles in the HDN of those aromatic heterocyclic nitrogen compounds. Fig. 7 presents the energy levels of the highest occupied and lowest unoccupied π-orbitals of different heterocyclic aromatic nitrogen compounds. These results show that the energy levels of the highest occupied π-orbital and the lowest unoccupied π-orbital for non-basic nitrogen compounds are higher than that for corresponding basic nitrogen compounds. The difference in electronic structures between basic and non-basic nitrogen compounds implies that transferring electrons from nitrogen compounds to the catalyst surface is easier for non-basic nitrogen compounds than for basic nitrogen compounds, and transferring electrons from the catalyst surface to nitrogen compounds is easier for basic nitrogen compounds than for non-basic nitrogen compounds. Therefore, the relative hydrogenation reactivities of basic and non-basic nitrogen compounds may vary depending on the electronic structures and properties of catalyst surfaces. On a catalyst surface with a strong ability of accepting electrons, non-basic nitrogen compounds may show higher reactivity, whereas on a catalyst surface with a strong ability of donating electrons, basic nitrogen compounds may be more reactive.

4. Conclusions

The negative Mulliken charges on the nitrogen atoms in the saturated nitrogen compounds determine their HDN reactivities on hydrotreating catalyst. The molecules with nitrogen atoms having higher negative Mulliken charges show higher HDN reactivities. For the hydrogenation of aromatic molecules, their reactivities are related to the energy levels of occupied or unoccupied π-orbitals. On unpromoted molybdenum catalysts, the occupied orbitals are important because the catalyst active sites have strong ability of accepting electrons and relatively poor ability of donating electrons. On Ni-promoted catalysts, the unoccupied orbitals are critical because the catalyst active sites have a strong ability of donating electrons and very poor ability of accepting electrons. Non-basic nitrogen compounds have higher energy π-orbitals than basic nitrogen compounds. Therefore, non-basic nitrogen compounds might be more reactive than basic compounds on a catalyst surface with a high density of unoccupied states, while the opposite may be true on a catalyst surface with a low density of occupied states.

Acknowledgements

This work is supported by Syncrude Canada Ltd. and the Natural Sciences and Engineering Research Council (NSERC) under grant no. CRDPJ 261129.

References

[1] R. Prins, V.H.J. de Beer, G.A. Somorjai, Catal. Rev.-Sci. Eng. 31 (1989) 1.
[2] H. Topsøe, B.S. Clausen, F.E. Massoth, Hydrotreating Catalysis Science and Technology, Springer Verlag, Berlin, 1996.
[3] T. Kabe, A. Ishihara, W. Qian, Hydrodesulfurization and Hydrodenitrogenation, Wiley–VCH, New York, 1999.
[4] J.F. Cocchetto, C.N. Satterfield, Ind. Eng. Chem., Process Des. Dev. (1976) 15.
[5] R. Prins, Adv. Catal. 46 (2001) 399.
[6] N. Nelson, R.B. Levy, J. Catal. 58 (1979) 485.
[7] R.M. Laine, Catal. Rev.-Sci. Eng. 25 (1983) 459.
[8] G. Perot, Catal. Today 10 (1991) 447.
[9] J.L. Portefaix, M. Cattenot, M. Guerriche, M. Breysse, Catal. Lett. 9 (1991) 127.
[10] J.L. Portefaix, M. Cattenot, M. Guerriche, J. Thivolle-Cazat, M. Breysse, Catal. Today 10 (1991) 473.
[11] L. Vivier, V. Dominguez, G. Perot, S. Kasztelan, J. Mol. Catal. 67 (1991) 267.
[12] M. Cattenot, J.L. Portefaix, J. Afonso, M. Breysse, M. Lacroix, G. Perot, J. Catal. 173 (1998) 366.
[13] F. Rota, V.S. Ranade, R. Prins, J. Catal. 200 (2001) 389.
[14] F. Rota, V.S. Ranade, R. Prins, J. Catal. 202 (2001) 195.
[15] M. Egorova, Y. Zhao, P. Kulula, R. Prins, J. Catal. 206 (2002) 263.
[16] Y. Zhao, P. Kulula, R. Prins, J. Catal. 221 (2004) 441.
[17] Y. Zhao, R. Prins, J. Catal. 222 (2004) 532.
[18] B. Delley, J. Chem. Phys. 113 (2000) 7756.
[19] M. Sun, A.E. Nelson, J. Adjaye, J. Catal. 226 (2004) 32.
[20] M. Sun, A.E. Nelson, J. Adjaye, J. Catal. 226 (2004) 41.
[21] A.D.J. Becke, Chem. Phys. 88 (1988) 2547.
[22] J.P. Perdew, Y. Wang, Phys. Rev. B 45 (1992) 13244.
[23] W. Kohn, L.J. Sham, Phys. Rev. A 140 (1965) 113.
[24] P. Pulay, J. Comp. Chem. 3 (1982) 556.
[25] M.D. Segall, P.L.D. Lindan, M.J. Probert, C.J. Pickard, P.J. Hasnip, S.J. Clark, M.C. Payne, J. Phys.: Cond. Matt. 14 (2002) 2717.
[26] J.P. Perdew, J.A. Chevary, S.H. Vosko, K.A. Jackson, M.R. Pederson, D.J. Singh, C. Fiolhais, Phys. Rev. B 46 (1992) 6671.

[27] H.G. Mcllvried, Ind. Eng. Chem., Process Des. Dev. 10 (1971) 125.
[28] R.S. Mulliken, J. Chem. Phys. 23 (1955) 1833.
[29] J. Quartararo, S. Mignard, S. Kasztelan, Catal. Lett. 61 (1999) 167.
[30] P. Raybaud, J. Hafner, G. Kresse, S. Kasztelan, H. Toulhoat, J. Catal. 189 (2000) 129.
[31] P. Raybaud, J. Hafner, G. Kresse, S. Kasztelan, H. Toulhoat, J. Catal. 190 (2000) 128.
[32] W. Kanda, I. Siu, J. Adjaye, A.E. Nelson, M.R. Gray, Energy Fuels 18 (2004) 539.
[33] P.G. Parr, W. Yang, Density-Function Theory of Atoms and Molecules, Oxford University Press, New York, 1989.